

Universal mechanism for Anderson and weak localization

Marcel Filoche^{a,b,1} and Svitlana Mayboroda^c

^aPhysique de la Matière Condensée, Ecole Polytechnique, Centre National de la Recherche Scientifique, 91128 Palaiseau, France; ^bCentre de Mathématiques et de Leurs Applications, Ecole Normale Supérieure de Cachan, Centre National de la Recherche Scientifique, UniverSud, 94230 Cachan, France; and ^cSchool of Mathematics, University of Minnesota, Minneapolis, 55455 MN

Edited by Michael Berry, University of Bristol, Bristol, United Kingdom, and approved July 20, 2012 (received for review December 13, 2011)

Localization of stationary waves occurs in a large variety of vibrating systems, whether mechanical, acoustical, optical, or quantum. It is induced by the presence of an inhomogeneous medium, a complex geometry, or a quenched disorder. One of its most striking and famous manifestations is Anderson localization, responsible for instance for the metal-insulator transition in disordered alloys. Yet, despite an enormous body of related literature, a clear and unified picture of localization is still to be found, as well as the exact relationship between its many manifestations. In this paper, we demonstrate that both Anderson and weak localizations originate from the same universal mechanism, acting on any type of vibration, in any dimension, and for any domain shape. This mechanism partitions the system into weakly coupled subregions. The boundaries of these subregions correspond to the valleys of a hidden landscape that emerges from the interplay between the wave operator and the system geometry. The height of the landscape along its valleys determines the strength of the coupling between the subregions. The landscape and its impact on localization can be determined rigorously by solving one special boundary problem. This theory allows one to predict the localization properties, the confining regions, and to estimate the energy of the vibrational eigenmodes through the properties of one geometrical object. In particular, Anderson localization can be understood as a special case of weak localization in a very rough landscape.

vibrations | eigenfunctions | elliptic operator | confinement

A puzzling feature exhibited by complex, irregular, or inhomogeneous systems is their ability to maintain standing waves or vibrations in a very restricted subregion of their domain even in the absence of confining force or potential. The most striking manifestation of this phenomenon is the famous Anderson localization which has fascinated scientists and spurred an extraordinarily abundant wealth of literature in the past 50 years (1–6). Since Anderson's seminal work in 1958 it is known that a sufficiently large structural disorder can lead to strongly localized quantum states, which are standing waves of the Schrödinger equation. This phenomenon has now been experimentally demonstrated in optic or electromagnetic systems (7–9).

Another well-known example of vibration confinement is the weak localization occurring in domains of irregular geometry and characterized by a slow decay of the vibration amplitude away from its main existence subregion (10–13), as opposed to the exponential decay of Anderson localization.

Considerable progress has been made to understand the onset of weak and Anderson localization, as well as the possible link between these two types of localization (14). Even though a few approaches statistically relate the energy levels to the potential in disordered solids (15, 16), there has been no general theory able to directly determine for any domain and any type of inhomogeneity the precise relationship between the geometry of the domain, the nature of the disorder, and the localization of vibrations, to predict in which subregions one can expect localized standing waves to appear, and in which frequency range.

Consider for instance a simple case of Anderson localization illustrated in Fig. 1. The original domain (called Ω) is a unit square. It is divided into $400 = 20 \times 20$ smaller squares. On each of these smaller squares, the potential $V(\vec{x})$ is constant, its value being determined at random uniformly between 0 and V_{\max} (here $V_{\max} = 8,000$, see Fig. 1, *Left*). We compute the quantum states, i.e., the eigenmodes ψ and the energy levels E of the Hamiltonian $H = -\Delta + V$ (the arbitrary energy units are taken such that $\hbar^2/2m = 1$). These quantum states obey the stationary Schrödinger equation with Dirichlet boundary conditions [Anderson's original paper used a tight-binding model which can be seen as the discrete projection of a continuous Hamiltonian, both converging toward the white noise potential in the limit of small lattice parameter (2)], as follows:

$$(-\Delta + V)\psi = E\psi \quad \text{in } \Omega, \quad \psi|_{\partial\Omega} = 0. \quad [1]$$

The five quantum states of lowest energy are plotted together in Fig. 1, *Right*. It appears that one cannot directly deduce the detailed shape of the localized quantum states, i.e., the boundary of the subregion that contains most of the mode energy, from the shape of the potential itself. Normally, one would have to solve the eigenvalue problem to retrieve this information.

In the present paper, we introduce a fundamentally unique theory that determines the localization subregions from the knowledge of the disordered potential itself. Unifying weak and Anderson localization within the same mathematical framework, the proposed theory reveals inside any vibrating system a hidden landscape that divides the original domain into several weakly coupled vibrating subregions. It unravels the relationship between the geometry of these localization subregions and the mode energy, and finally predicts the critical energy above which one can expect fully delocalized, i.e., conducting states to appear.

Results

The Landscape of Localization. The essential step in our approach consists in solving not the eigenvalue problem, but the Dirichlet problem with uniform right-hand side and Dirichlet boundary conditions, as follows:

$$(-\Delta + V)u = 1 \quad \text{with } u|_{\partial\Omega} = 0. \quad [2]$$

The Hamiltonian $H = -\Delta + V$ is a second-order elliptic operator with variable coefficients, which is positive if $V(\vec{x})$ is positive everywhere. In this case the solution u is a positive function, and its map can be considered as a landscape (see Fig. 2, *Left*)

Author contributions: M.F. and S.M. designed research; M.F. and S.M. performed research; and M.F. and S.M. wrote the paper.

The authors declare no conflict of interest.

This article is a PNAS Direct Submission.

¹To whom correspondence should be addressed. E-mail: marcel.filoche@polytechnique.edu.

This article contains supporting information online at www.pnas.org/lookup/suppl/doi:10.1073/pnas.1120432109/-DCSupplemental.

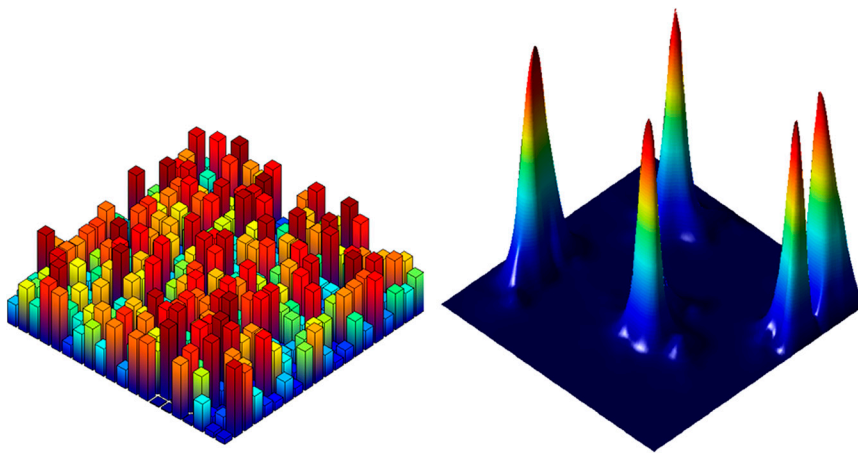


Fig. 1. (Left) Three-dimensional view of the random potential $V(\vec{x})$ entering the Schrödinger equation. The square domain is divided in 20×20 smaller squares. In each small square, the potential V is assigned an independent random value uniformly distributed between 0 and V_{\max} (here 8,000). (Right) Three-dimensional view of the fundamental and the first four excited states. From the view of the potential only, it seems impossible to predict the localization regions and the spatial distribution of these states.

characterized by a complex relief with many valleys and peaks. In particular, one can draw in this landscape the network of interconnected valleys of varying depths. Using the streamlines of this landscape as guidelines, the corresponding valleys are delineated in Fig. 2, *Middle*. The thickest lines represent the deepest valleys, whereas the moderately thick lines correspond to the shallower ones. This intricate network reveals a complex partition of the domain into numerous subregions that was impossible to guess by just looking at the random potential at hand.

If one now superimposes the valley network on top of the three-dimensional (3D) representation of the eigenmodes (Fig. 2, *Right*), one can observe how accurately these lines predict the localization subregions of the different modes. The reason for this accurate prediction is that every eigenmode ψ satisfies the following identity (*SI Appendix* gives the mathematical proof):

$$|\psi(\vec{x})| \leq Eu(\vec{x}), \quad \text{for all } \vec{x} \text{ in } \Omega. \quad [3]$$

Here E is the mode energy, ψ is the mode amplitude normalized so that $\sup_{\Omega} |\psi| = 1$, and $u(\vec{x})$ is the landscape defined above in Eq. 2, i.e., a function independent of the eigenmode ψ . One can add here that for complex Hamiltonians (containing for instance magnetic interaction), one can obtain a more general definition of the function $u(\vec{x})$ that always leads to a nonnegative real-valued function. This expression will be given later in the paper.

Through inequality [3], the function u compels the eigenmodes to be small along its lines of local minima, i.e., along the valleys of the landscape displayed in Fig. 2, *Middle*. These valleys are de-

fined as the lines of steepest descent, starting from the saddle points of the landscape and going to its minima. These lines also can be seen as antwatersheds, in other words the watershed lines of the reversed landscape. The network formed by these valleys, a priori invisible when looking at the domain but clearly identifiable on the graph of u , operates as a driving force that determines the confinement properties.

The Effective Valley Network. Whereas the network of valleys is determined by u and is independent of the eigenmodes, the strength of the confinement of an eigenmode dictated by inequality [3] diminishes as the energy E increases. Given the normalization chosen for the eigenmodes, this inequality represents an effective constraint only at those points $\{\vec{x}\}$ where $Eu(\vec{x})$ is smaller than 1. In other words, an eigenmode of energy E can only actually see, or be constrained by, the portion of the initial valley network where $u(\vec{x}) < 1/E$. This subset of the entire network, parameterized by E , is referred to as the effective valley network $\mathcal{N}(E)$.

From its definition, it is immediate to see that if $E' > E$ the effective valley network $\mathcal{N}(E')$ is a subset of the effective valley network $\mathcal{N}(E)$. In other words, the family of effective networks $[\mathcal{N}(E)]_{0 \leq E < +\infty}$ constitutes a decreasing sequence of sets as E increases. For $E = 0$, the effective valley network $\mathcal{N}(0)$ is simply the entire original valley network, whereas, when E goes to infinity, the network $\mathcal{N}(E)$ progressively disappears entirely.

To observe how the effective valley network drives the confinement of the eigenmodes, we plot the amplitude of a number of modes (or quantum states) at lower and higher energies (Fig. 3).

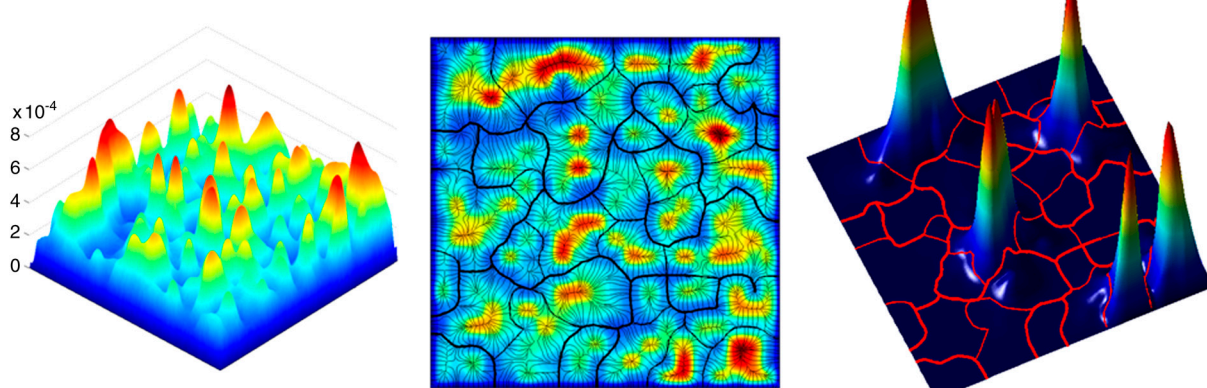


Fig. 2. (Left) Three-dimensional view of the landscape of u , obtained by solving $[-\Delta + V(\vec{x})]u = 1$. (Middle) Two-dimensional color representation of the map of u , together with the streamlines and valleys. The very thin lines correspond to the streamlines, the thicker lines correspond to the deepest valleys, and the moderately thick lines to the more shallow ones. This landscape draws an intricate network of interconnected valleys. One can conjecture that in the limit of a Brownian potential, this network becomes scale invariant and exhibit fractal properties. (Right) Network of the valleys deduced from the middle figure superimposed with the first five eigenmodes of the domain. One can observe how the network accurately defines the subregions that enclose the modes.

For each mode of energy E , the corresponding effective valley network $\mathcal{N}(E)$ is plotted on top of the mode amplitude. It is striking to see how all modes are clearly shaped by this network. The fundamental and the first excited states (modes 1 to 8) are completely localized in one of the subregions bounded by the valley lines. At higher energies (mode 45, 48, 70), the effective valley network begins to shrink, opening breaches in the shallowest valley lines. Consequently, subregions that were initially disjoint progressively merge to form larger subregions. One can observe that the corresponding modes are still localized, but now exactly in the much larger subregions defined by the remaining effective network. Still, some small subregions remain in which one can find localized modes weakly coupled to the rest of the domain (modes 47 and 71). At even higher energies (modes 97–99), a transition occurs: The effective valley network is mostly disconnected allowing subregions to percolate throughout the entire domain: Fully delocalized states can now appear.

For sake of simplicity, simulations have been carried out in two dimension (2D). In 3D or larger dimensions, the valleys would not be lines but surfaces where u is locally minimal, and the entire valley network would take the shape of a foam which separates the domain into a large number of subregions. When the energy

increases, the effective valley network $\mathcal{N}(E)$ would shrink by opening gaps in the walls separating adjacent subregions.

One can examine in detail the strength of the localization by plotting the mode amplitude on a logarithmic scale (Fig. 4). By doing so, one can notice that the level curves are on average equally spaced, which corresponds to an exponential decay away from the existence subregion. More precisely, we observe again our landscape at work: The amplitude of the mode is approximately of the same order of magnitude inside each subregion. The decay of the eigenmode essentially occurs each time a boundary between two adjacent subregions is crossed (this boundary corresponds to a valley line of the landscape). This effect is particularly clear for the two modes in Fig. 4 in which their principal existence subregion appears dark red, all nearest neighboring subregions appear light red, further subregions essentially orange, etc. Therefore, each subregion is weakly coupled to its neighbors, the mode decaying by a somewhat constant factor each time it crosses a valley line away from the center subregion of existence. When zoomed in on any of these subregions, the mode localization is of the weak type. However, because of the intricacy of the valley network, the succession of regularly spaced valley lines in the effective network yields an exponential decay of

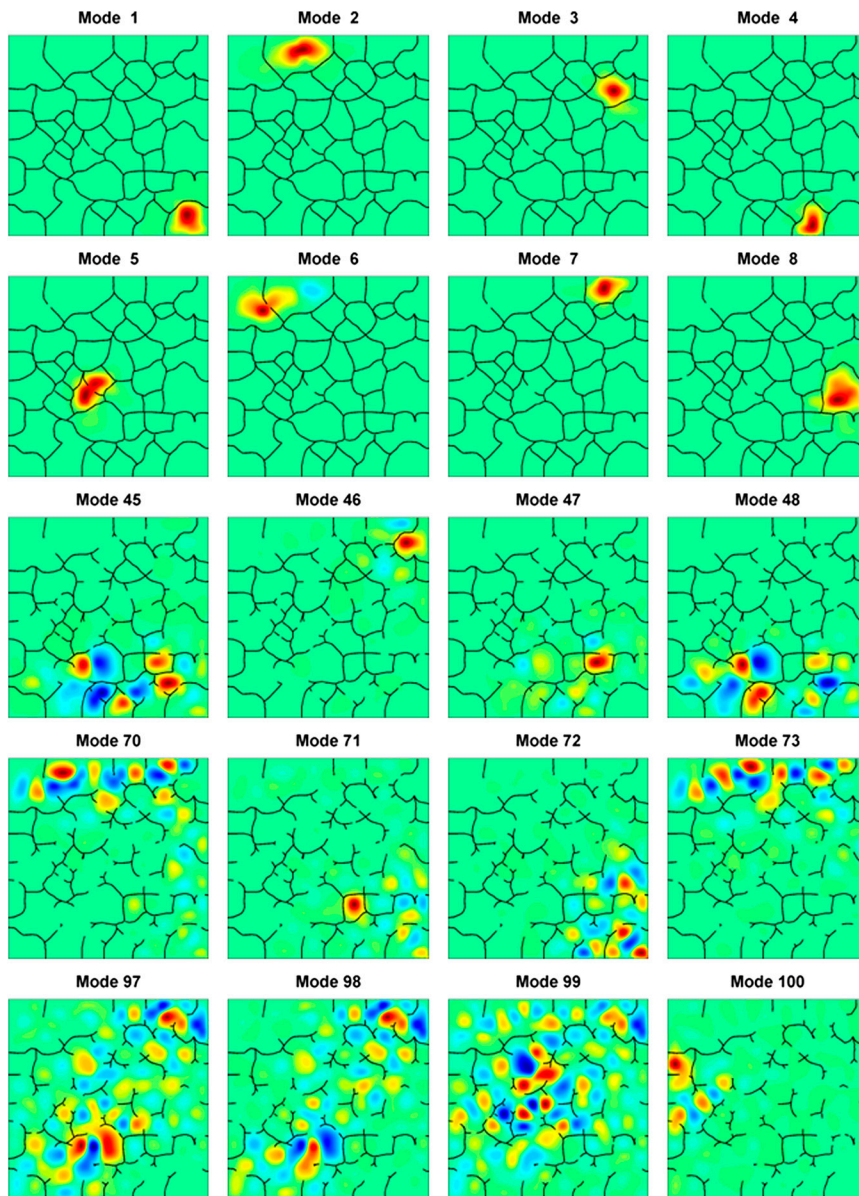


Fig. 3. Spatial distribution of several quantum states in the random potential of Fig. 2. On top of each state is drawn the effective valley network corresponding to the state energy. One can clearly observe that all modes are localized exactly in one of the subregions delimited by the effective valley network.

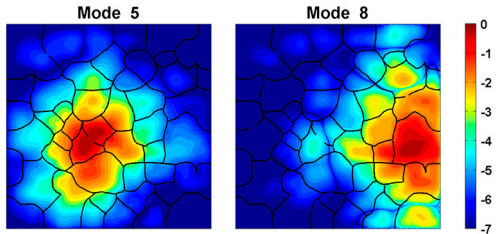


Fig. 4. Logarithmic plot (in log10) of the amplitude for two excited states in the potential shown in Fig. 2. One can observe here in detail how strong localization emerges from weak localization. Both modes are located in one of the subregions delimited by the valley ways. Moreover, their decay is shaped by neighboring subregions. First, the mode amplitude is more or less uniform within any subregion. Second, when going away from the main subregion, crossing a valley line corresponds to a decrease by one or two orders of magnitude. Successive decreases lead to an exponential decay for distances substantially larger than the typical size of a subregion.

the mode away from its center subregion, over distances much larger than the typical size of a subregion. As a consequence, the mode appears to be exponentially confined: Strong localization emerges from successive and cumulative weak localizations.

Applying our theory in one dimension (1D) gives a very straightforward interpretation of how Anderson localization operates. The valleys are reduced in this case to single points, which are by definition the local minima of the function $u(x)$. The localization subregions are the intervals separating two successive points and the strength of the localization is determined by the values of $u(x)$ at these separation points. From this geometrical interpretation of localization, it is immediately intuitive that it is much easier to form localization subregions in 1D, only bounded by two points, than in 2D or 3D where it requires a closed line or a closed surface.

The Formation of Localized Modes. From the previous section, it clearly appears that the effective valley network deduced from inequality [3] thoroughly controls the localization properties. However, this inequality efficiently constraints the mode amplitude along the valleys of the landscape only. How is it possible that a constraint exerted along a boundary line suppresses the vibration outside the localization subregion?

Consider a subregion Ω_1 of the original domain Ω carved out by the valley lines of the landscape of u . It can be thought of, for instance, as any of the subregions in Fig. 2, *Right*. By construction, the function u is relatively small (locally minimal) along the boundary of Ω_1 . Thus, for lower values of the energy E , the inequality [3] provides a severe constraint on the mode amplitude ψ along the boundary $\partial\Omega_1$. As a result, any eigenmode ψ of the entire domain can locally be viewed as a solution to the problem

$$H\psi = E\psi \quad \text{in } \Omega_1, \quad [4]$$

$$\psi = 0 \quad \text{on } \partial\Omega_1 \cap \partial\Omega \quad \text{and} \quad \psi = \varepsilon \quad \text{on } \partial\Omega_1 \setminus \partial\Omega, \quad [5]$$

where $\varepsilon(\vec{x})$ is a quantity smaller than $Eu(\vec{x})$ on the boundary of Ω_1 . Observe that the boundary value problem [4, 5] is, in fact, akin to the eigenvalue problem in the subregion Ω_1 alone: The differential equation inside the subregion is identical, but on the boundary ψ is small in Eq. 5 rather than just being zero, as an eigenvalue problem on Ω_1 would normally warrant.

Any eigenmode ψ satisfying the above boundary problem also satisfies the following inequality, which plays an essential role in understanding the origin of localization (*SI Appendix* gives the mathematical proof):

$$\|\psi\|_{L^2(\Omega_1)} \leq \left(1 + \frac{E}{d_{\Omega_1}(E)}\right)\|\varepsilon\|. \quad [6]$$

Here, $d_{\Omega_1}(E)$ is the distance from E to the spectrum of the Hamiltonian H in the subregion Ω_1 only. This distance is defined as $d_{\Omega_1}(E) = \min_{E_{i,\Omega_1}} |E - E_{i,\Omega_1}|$, the minimum being taken over all energies (E_{i,Ω_1}) of H in Ω_1 only. The norm $\|\varepsilon\|$ is the L^2 -norm of the solution to $Hv = 0$ in Ω_1 with data ε on $\partial\Omega_1$ (in the sense of Eq. 5). In particular, $\|\varepsilon\|$ becomes arbitrarily small as ε vanishes.

This inequality can be understood in fairly simple terms. If ε is identically zero, it implies that ψ can be nonzero in the subregion Ω_1 only if its energy exactly matches one of the energies E_{i,Ω_1} of the spectrum of H in Ω_1 .

If ε is nonidentically zero, the presence of $d_{\Omega_1}(E)$ in the denominator of the right-hand side of Eq. 6 assures that whenever E is far from any eigenvalue of H in Ω_1 in relative value, the norm of ψ in the entire subregion Ω_1 has to be smaller than a quantity of the order of $\|\varepsilon\|$. Consequently, such a mode ψ is expelled from Ω_1 and must live in its complement.

Conversely, the mode ψ can only be substantial in the subregion Ω_1 when its energy E almost coincides with one of local eigenvalues of the operator H in Ω_1 . In that case Eq. 4 yields the conclusion that ψ itself almost coincides with the corresponding eigenmode of the subregion Ω_1 .

Thus, we obtain a rigorous scheme elucidating the formation of weak localization. In any subregion delimited by the valleys of u , an eigenmode of Ω has only two possible choices: (i) its amplitude is very small throughout this subregion, or (ii) this mode mimics (both in frequency and in shape) one of the subregion's own eigenmodes. Consequently, a low frequency eigenmode can cross the boundary between two adjacent subregions only if they possess two similar local eigenvalues. More generally, a fully delocalized eigenmode can only emerge in this context through one of the two possibilities. Either the mode is a collection of local eigenmodes of the subdomains sharing a common eigenvalue, or the effective valley network has shrunk enough to allow a passage throughout the domain. The former corresponds to Bloch waves whereas the latter corresponds to delocalization above Anderson transition (17–19).

Toward a General Theory of Localization. Although the mathematical theory of localization described above was illustrated through Anderson localization, its range of validity is much wider. In fact, it can be applied to treat low frequency localization, for any type of vibration, any medium, any domain geometry, and any dimension.

In very general terms, a vibrating system is governed by a wave equation associated to a suitable elliptic differential operator L . The latter is determined by the nature of vibration and the medium. For instance, the Laplacian $L = -\Delta$ is used to describe the vibration of a bidimensional soft membrane, the propagation of acoustic waves, or the quantum states inside a box or cavity; variable coefficient second-order operators $L = -\operatorname{div}[A(x)\nabla]$ pertain to the aforementioned phenomena in inhomogeneous media; and the bi-Laplacian Δ^2 addresses thin plate vibrations in 2D. In our study of Anderson localization, the operator L was the Hamiltonian H . The standing waves ψ are therefore eigenmodes of this operator with eigenvalue λ , also called frequency (λ being the generalization of the energy E).

The very general definition of the landscape u is the as follows (*SI Appendix* gives the mathematical proof):

$$u(\vec{x}) = \int_{\Omega} |G(\vec{x}, \vec{y})| dy, \quad [7]$$

where $G(\vec{x}, \vec{y})$ is the Green's function solving $LG(\vec{x}, \vec{y}) = \delta_{\vec{x}}(\vec{y})$ with zero data on the boundary. (For the sake of brevity, we assume Dirichlet boundary data. Other types of boundary conditions will be addressed in forthcoming publications).

It is interesting to note that, for all second-order differential operators, the Green's function is positive. In that case u admits

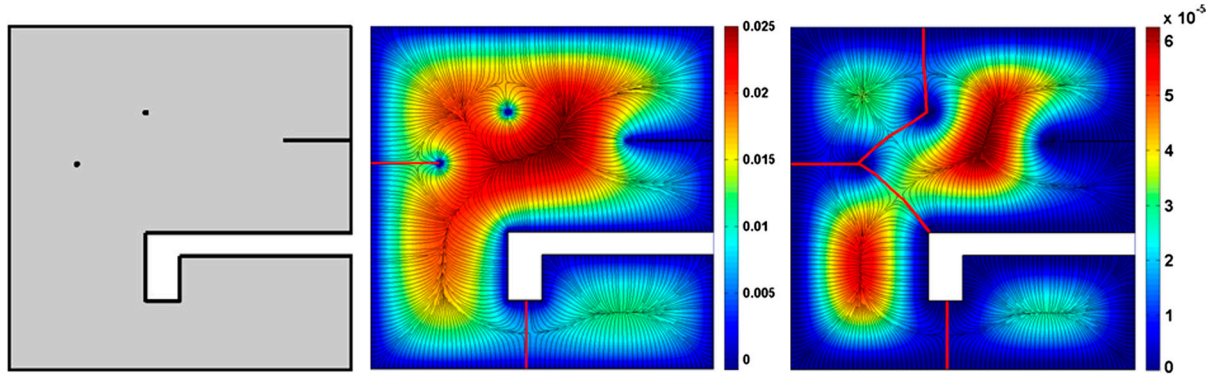


Fig. 5. (Left) Geometry of a complex domain, with a bottleneck (in the lower part), two inner blocked points, and an inward crack (on the upper right side). The question is, as follows: Is there localization in this structure? Which modes will be localized and where? (Middle and Right) Two-dimensional representations of the landscape u for the Laplacian (Middle) and the bi-Laplacian (Right) in the same domain. The colors correspond to the height of the landscape. The (thin black) streamlines help to detect the valley lines, which are then highlighted as thick red curves. These valleys delimit two subregions of localization for the Laplacian and four subregions for the bi-Laplacian.

a remarkably simple definition. It is the solution to the Dirichlet problem

$$Lu = 1 \quad \text{in } \Omega, \quad u|_{\partial\Omega} = 0, \quad [8]$$

which is exactly the equation used to obtain the landscape u in Anderson localization. In physical terms, the function u can be interpreted, for instance, as the steady-state deformation of a membrane under a uniform load.

In the general case however, if G is complex-valued (e.g., a Hamiltonian with magnetic interaction) the function in Eq. 7 does not solve Eq. 8. Eq. 7 can then be directly used to determine the main landscape of our theory.

Let us now illustrate an application of our theory to weak localization induced by the domain geometry. Consider, for instance, the domain depicted in Fig. 5, *Left*. It has a nontrivial shape, possesses two inner blocked points (in the upper left region), one crack on the right upper boundary, and a bottleneck in its lower region. This domain can represent either a flexible membrane of complex shape (the differential operator being then the Laplacian), or a rigid thin plate (the operator being the bi-Laplacian). Fig. 5 displays two maps of u computed in the same complicated geometry for the Laplacian (*Middle*) and the bi-Laplacian (*Right*), respectively. The streamlines (lines of the gradient) have been plotted in thin black to clearly pinpoint the valleys, which are highlighted as thick red lines. The two cases expose dramatically different patterns. For the Laplacian, one can observe two valleys, and only one of them splits the domain into two disjoint subregions. In the bi-Laplacian case, five valleys form a network yielding a partition of the domain into four disjoint subregions.

One can now observe in these two examples how the valleys of u govern the appearance of localization. Fig. 6, *Left*, displays two localized modes (number 1 and 5) of the Laplacian plotted together with the valley lines computed in Fig. 5, *Middle*. Not only do these modes obey the pattern predicted by the landscape u , but there exists no eigenmode confined to a smaller subregion. In Fig. 6, *Right*, modes 1, 2, 4, and 6 of the bi-Laplacian are displayed in the same domain together with the valley lines from Fig. 5, *Right*. We observe here a very different and much larger variety of localization behaviors. However, once again, the location, the shape, and the number of the localization subregions exactly match the partition of the domain generated by the valley network of the landscape u computed in Fig. 5.

Discussion

Our theory unifies both weak and Anderson localization as two manifestations of the same phenomenon of low frequency loca-

lization. Above a critical frequency (or eigenvalue), delocalized states can exist, and this critical value is the smallest frequency λ_c for which a sufficient proportion of the valley lines of u have disappeared so that the effective valley network $\mathcal{N}(\lambda_c)$ allows one subregion to percolate throughout the system. Remarkably, computing the landscape of u and the effective valley network at any frequency does not require any a priori knowledge of the quantum states or stationary vibrations of the system, but yet gives access to accurate information on the confinement of the states within any frequency range. One should note that the same mathematical theory can be applied to a discrete wave operator defined on a lattice (as for instance in the tight binding model of a finite system), only replacing integrals and scalar products by finite sums.

Note also that the precise quantitative information on evolution of the effective network $\mathcal{N}(\lambda)$ with the growth of the eigenvalue λ is already encoded in the original mapping of u . In this vein, it would be extremely useful to estimate precisely the underlying rate of growth of the eigenvalues. Roughly speaking Weyl's law (20) predicts that for any given $\lambda > 0$ the number of the eigenvalues of L below λ is asymptotically $\lambda^{d/2m}$, where d stands for the dimension and $2m$ is the order of the differential operator L . This estimate can be employed in the present context to determine the range of frequencies with high response to the impact of u , that is, the range of thoroughly localized eigenmodes. Moreover, although the proposed theory primarily accounts for low

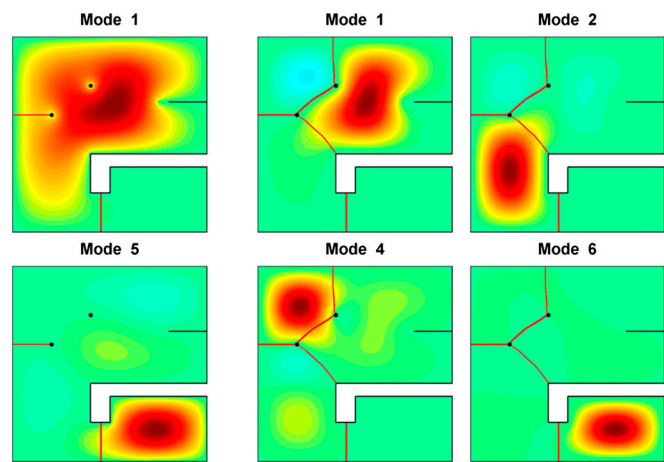


Fig. 6. Two localized modes of the Laplace operator (*Left*) and four localized modes of the bi-Laplace operator (*Right*). In both cases, the valley network (displayed in red) obtained in Fig. 5 accurately predicts the number and the location of the localization subregions.

frequency localization, in a domain of self-similar boundary, smaller copies of the valley lines would appear at all scales, triggering mode localization for an infinite number of eigenvalues. In that case one would always find localized modes in the high frequency limit governed by Weyl's law.

Also, the scaling theory of localization can be reformulated in geometrical terms. In the corrugated landscape created by a random potential, the existence of delocalized modes will crucially depend on the existence of matching energies for distant subregions, and therefore on the asymptotic shape of the distribution of subregion sizes. As this distribution is expected to strongly depend on the dimensionality of the system, one can hope to derive a geometrical criterion for the delocalization transition as a function of the spatial dimension.

At this point, it is important to note that this unifying scheme for weak and Anderson localization does not include the scar localization that occurs at high frequency near the stable periodic orbits or geodesics of the domain. There are two important differences between the scar modes and the localization investigated in the present paper (weak localization and Anderson localization). First, the scar modes occur at high frequencies whereas weak localization and Anderson localization are low frequency phenomena. Secondly, the type of localization that we address in this paper is local in the sense that a localized mode in a given subregion is not strongly influenced by far remote details of the domain geometry or remote inhomogeneities of the potential. In sharp contrast, the scar mode localization heavily depends on the delicate and coherent interaction between very distant regions of the domain boundary to build stable orbits. The localization subregions in this case are very narrow but span the entire domain.

Finally, one should add that, although the landscape u in Anderson localization is obtained by simply solving one linear system, it nevertheless depends in a complex way upon the quenched disorder. In particular, different types of randomness would lead to different localization properties. More generally, the question of localization in any disordered or random system can now be mathematically reformulated in the following simple way: How does the valley network of the landscape of u (its connectivity, density, and height), depend on the properties of the disorder? For instance, localization of the conduction electrons directly affects the transport properties of a disordered medium (21). At zero temperature, such a medium is insulating if all occupied quantum states are localized. With the theory proposed in this paper, this condition can now be reformulated and studied in terms of the percolation properties of the effective valley network at the energy equal to the Fermi level of the system.

Conclusion

Our findings demonstrate that low frequency localization is a universal phenomenon, observed for any type of vibration governed

by a spatial differential operator L that derives from an energy form. The geometry of the domain and the properties of the operator interplay to create a landscape u which entirely determines the localization properties of the system. First, its network of valley lines (in 2D) or surfaces (in 3D) generates an invisible partition of the initial domain, which shape the spatial distributions of the vibrational modes and precisely identify the subregions confining the vibrations. Second, the depth of these valleys determines the strength of the confinement within each subregion. The localization of a given mode of eigenvalue λ is in fact controlled by an effective valley network $\mathcal{N}(\lambda)$ defined as the subset of the entire original valley network subject to the condition $u < 1/\lambda$. Consequently, the relative number of localized modes decreases at high frequencies. A complex vibrational system can thus be understood as a collection of weakly coupled subregions whose coupling increases with frequency.

The theory holds for systems of irregular geometry as well as for disordered ones. In this framework, Anderson localization arises as a specific form of weak localization, strengthened by the extremely rough landscape generated by the random potential. More generally, the macroscopic properties of materials or systems in which localization plays an essential role can now be reformulated from the geometrical and analytical characteristics of the effective valley network.

This theory of localization opens a number of problems. In the case of domain with fractal boundary, can one relate the asymptotic distribution of eigenmodes with the scaling properties of the valley network? Can one deduce the thermodynamical behavior of noninteracting bosons or fermions in a disordered system from the knowledge of the effective valley network at every energy? What are the statistical properties of the landscape of u in a system of N interacting particles?

Finally, one should stress that the effective valley network $\mathcal{N}(\lambda)$ is promising to become a unique tool of primary importance for designing systems with specific vibrational properties. To this end, future studies should investigate in detail the relationship between the geometry of a system (irregular or fractal), the characteristics of the wave operator (order, nonhomogeneity, possibly stochastic), and the properties of one key mapping, the resulting valley network.

ACKNOWLEDGMENTS. The authors thank Guy David for fruitful discussions. Part of this work was completed during the visit of S.M. to the Ecole Normale Supérieure (ENS) de Cachan. Both authors were partially supported by the ENS Cachan through the Farman program. M.F. is also partially supported by the ANR Program Silent Wall ANR-06-MAPR-00-18. S.M. is partially supported by the Alfred P. Sloan Fellowship, the NSF CAREER Award DMS 1056004, NSF Grant DMS 0758500, and NSF Materials Research Science and Engineering Center Seed grant.

- Anderson PW (1958) Absence of diffusion in certain random lattices. *Phys Rev* 109:1492–1505.
- Thouless DJ (1974) Electrons in disordered systems and the theory of localization. *Phys Rep* 13:93–142.
- Abrahams E, et al. (1979) Scaling theory of localization: Absence of quantum diffusion in two dimensions. *Phys Rev Lett* 42:673–676.
- Lee PA, Ramakrishnan TV (1985) Disordered electronic systems. *Rev Mod Phys* 57:287–337.
- Evers F, Mirlin AD (2008) Anderson transitions. *Rev Mod Phys* 80:1355–1417.
- Lagendijk A, van Tiggelen B, Wiersma DS (2009) Fifty years of Anderson localization. *Phys Today* 62:24–29.
- Laurent D, Legrand O, Sebbah P, Vanneste C, Mortessagne F (2007) Localized modes in a finite-size open disordered microwave cavity. *Phys Rev Lett* 99:253902.
- Sapienza L, et al. (2010) Cavity quantum electrodynamics with Anderson-localized modes. *Science* 327:1352–1355.
- Riboli F, et al. (2011) Anderson localization of near-visible light in two dimensions. *Opt Lett* 36:127–129.
- Heilmann S, Strichartz R (2010) Localized eigenfunctions: Here you see them, there you don't. *Notices Amer Math Soc* 57:624–629.
- Baranger H, Jalabert R, Stone A (1993) Weak-localization and integrability in ballistic cavities. *Phys Rev Lett* 70:3876–3879.
- Félix S, Asch M, Filoche M, Sapoval B (2007) Localization and increased damping in irregular acoustical cavities. *J Sound Vib* 299:965–976.
- Filoche M, Mayboroda S (2009) Strong localization induced by one clamped point in thin plate vibrations. *Phys Rev Lett* 103:254301.
- Aizenman M (1994) Localization at weak disorder—some elementary bounds. *Rev Math Phys* 6:1163–1182.
- Lifshitz IM (1964) The energy spectrum of disordered systems. *Adv Phys* 13:483–536.
- Thouless DJ, Elzain ME (1978) The two-dimensional white noise problem and localization in an inversion layer. *J Phys C Solid State Phys* 11:3425–3438.
- Zhang ZQ, et al. (1999) Wave transport in random media: The ballistic to diffusive transition. *Phys Rev E* 60:4843–4850.
- Punnoose A, Finkel'stein AM (2005) Metal-insulator transition in disordered two-dimensional electron systems. *Science* 310:289–291.
- Richardella A, et al. (2010) Visualizing critical correlations near the metal-insulator transition in $Ga_{1-x}Mn_xAs$. *Science* 327:665–669.
- Weyl H (1911) On the asymptotic distribution of eigenvalues. *Göttinger Nachr* 1911:110–117 (in German).
- Wang J, Genack A (2011) Transport through modes in random media. *Nature* 471:345–348.